CONTROLLER DESIGN FOR HEAVY-HAUL TRAIN SYSTEM

M. Chou, X. Xia

Department of Electrical, Electronic and Computer Engineering, University of Pretoria, Pretoria, 0002, South Africa

Abstract: In this paper the existing control methods for train control in the various areas such as energy consumption and travelling time are examined. A closed-loop cruise controller to minimise the in-train force in the couplers is proposed. Simulation results for both regulation and disturbance rejection are given.

1. INTRODUCTION

The main strength of South African's export lies in its mineral exports, rare metals such as platinum and gold as well as energy source such as coal. As most mines are situated inland, heavy-load capable transportation system is required to move the minerals to the harbours. Interestingly, out of all the minerals, coal plays an important role, bringing R11 billion in foreign exchange in 2000/2001.

Coallink, the Spoornet railway from the coal-rich mines in Ermelo to the Richard's bay harbours carries over 60 million tons with its 200 wagon train. The increase in demands has resulted in the line running at full capacity. To increase revenue, the running cost of the existing trains has to be reduced.

The running cost of a train can be attributed to three main factors: energy consumption, travelling time and in-train forces. Numerous studies can be found for the first two factors as these are the dominant running cost factors for light passenger trains, such as the new high speed trains (HST). Some of the existing approaches are briefly explained in section 2. The last factor, in-train forces, is present in passenger train at an acceptable level. This, however, does not apply to heavy-haul trains.

In-train forces are the impact and stress forces experienced by the spring-like couplers that connect each car together in a train. Due to the extra long length and the heavy loads, in-train forces are significance in heavy-haul trains. This demands frequent maintenance and shorten service time for the couplers.

In the current pneumatic controlled brake system, signal propagation of the pressure wave used is limited to the speed of sound. Long delay results as the length of the train exceeded 2.5km. Due to this brake signal delay, the train experiences uneven braking whereby the front part of the train will brake before the end of the train. The reverse applies when brake is released. Another limitation was that the cars could not brake individually due to the way the brake pipe pressure is used for both brake signal transmission and brake force supply.

These factors hinder the performance of the brake system, resulting in increase in braking time and very large in-train forces.

The new electronic controlled pneumatic (ECP) brake system to be installed on the Coallink trains will provide control flexibility that was not possible with the existing pneumatically controlled brake system. The new ECP system replaces the pneumatic brake control with electronic signals, allowing almost simultaneous brake control by wire and individual brake setting for each car.

The actual brake force will still be applied pneumatically, only the control signal will be electronically transmitted. With its control flexibilities, the new ECP system makes it possible to implement dedicated cruise controllers that minimise in-train forces in addition to energy consumption.

This study is motivated by the need of the Spoornet Coallink system, but the approach as well as the technical train parameters are generic. This paper describes an early attempt to minimise the in-train forces by designing a cruise controller for the heavy-haul train. A state feedback controller is designed to regulates the velocities of the cars. Factors such as the velocity of each car and in-train forces of individual connectors are examined. It is shown that the controller improved the reference tracking performance and reduced the in-train force behaviours.

This paper is divided into two parts: Section 2 describes the existing control approaches in reducing energy consumption and travelling time of the train. Section 3 investigates the behaviours and control methods of in-train forces in detail; A generic model is used in conjunction with open-loop and closed-loop controllers.

2. EXISTING CONTROL METHODS

2.1 Optimal Control

In a scenario posed by Howlett (1996), an optimal control strategy for a diesel-powered passenger train was demonstrated. It was shown that the system was able to reduce the energy consumption while still complete the journey within certain time limit.

In an optimal strategy, a cost function is defined. In this case, it is based on the energy usage throughout the trip. The total distance is divided into subintervals via the switching points. Throughout the subintervals the velocity of the train will be constant until it reaches the next switching point.

To calculate the energy usage, predetermined information about the train and the railway track is required. The mass of the cars, locomotive traction power output, the brake force exerted by the locomotive and wagons are some of the train parameters needed. Track information, such as slope, degree of turns, track speed limits, are crucial both in calculating the energy usage as well as the placement of the switching points.

First, the optimal number and placement of the switching points will need to be determined for the given track. If there are more switching points, the more control points will be available. Mathematically, more available control points can lead to a more efficient control strategy. In practice, this is limited by the response time of the train and counterbalanced by the increase in computation time required for more complex systems.

Once the cost function and the position of the switching points are determined, calculation can be performed to obtain the optimal strategy. Interestingly, the results gave by Howlett (1996) support that speed-holding strategy is the most energy-efficient.

In practice the optimal control strategy suffers some deficiencies. Recalculation will have to be performed if some disturbances were experienced during the journey. Possible scenarios include stopping for additional wagons to be attached and emergency stops. Unpredictable factors such as weather conditions might also affect the performance of the optimal strategy.

Due to the aforementioned factors, optimal control is not reliable as the sole control method. Its result should still be considered as a guideline for other control methods for its inherited cost minimisation ability.

2.2 Maximum Adhesive control

A subtle but important control problem is the slip of the traction wheels. Slip, or slip velocity, of a wheel is defined as

$$slip = \omega r - v \tag{1}$$

where ω and r is the actual radial velocity and radius of the wheel and v is the linear velocity of the car.

Through experiments, it was found that the coefficient of friction between the wheel and the track is dependent on the slip velocity. This result was shown by Ishikawa and Kawamura (1997), shown in figure 1.

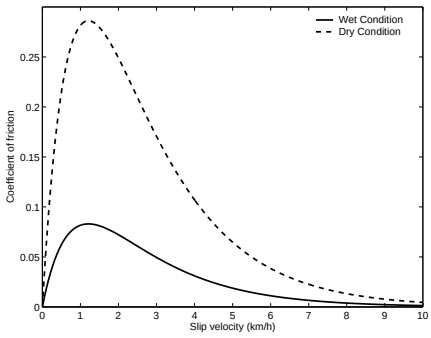

Fig. 1. Coefficient of friction versus the slip velocity

The aim is to keep the slip around the point that produces the maximum coefficient of friction, which in turn results in the maximum adhesive

force. To achieve this type of control, an accurate measurement of the wheel velocity is required. This is often difficult and expensive in practice due to the harsh environment found at the undercarriage. A novel wheel slip detector via the measurement of the changes in the traction motor current was shown by Watanabe and Yamashita (2001). As soon as a wheel slip passes the optimal point, the current to the traction motor would abruptly increase. Ishikawa and Kawamura (1997) demonstrated a PI-based controller that is able to maintain the slip velocity very closely around the optimal point.

3. IN-TRAIN FORCE CONTROL

This study attempts to minimise the in-train force by designing a cruise controller for the heavy-haul train. As found by Howlett (1996), speed-holding strategies proved to be most energy efficient, which further supports the choice of the cruise controller approach. This study adapts the the train model and the linearization method suggested by Yang and Sun (2001) and designs a state feedback controller for the given heavy-ore train system.

3.1 Train dynamics

The train model suggested by Yang and Sun (2001) places emphasis on the spring-like nature of the connectors, which increases the complexity of the model. This, in comparison with the simpler rigid body model, treats the velocity of every car individually, a necessity for in-train force analysis.

The train parameters adopted most of the parameters given in Yang and Sun (2001) since most parameters for the Spoornet Coallink trains are not yet available. The values are shown in table 1.

Table 1. Heavy-haul train parameters.

Parameter	Value	Unit
Number of wagons	4	
Locomotive mass	103250	kg
Wagon mass(Loaded)	104250	kg
K	$40 \sim 120 \times 10^3$	Nm^{-1}
C_0	0.01176	Nkg^{-1}
C_v	7.7616×10^{-4}	$Ns(mkg)^{-1}$
C_a	$1.6 \times 10{-}5$	$Ns^2(m^2kg)^{-1}$
V_0	$1 \times 10{-}5$	ms^{-1}

The connector behaviour is characterised by the spring coefficient K: a large spring coefficient results in a more rigid behaviour while a smaller spring coefficient causes more severe oscillation. To consider the worst case in the analysis, the lower end spring coefficient is used throughout the simulation.

The two major resistances experienced by a train are rolling resistance and aerodynamic drag. While the former is experienced by each car, the aerodynamic drag is only considered for the first car, often the locomotive. The general resistance is given as

$$R = \underbrace{c_0 + c_v v}_{R^r} + \underbrace{c_a v^2}_{R^a} \tag{2}$$

where v is the velocity of the car, R^r is the rolling resistance, R^a is the aerodynamic drag and the coefficients c_0, c_v, c_a are obtained experimentally.

Aerodynamic drag only becomes dominant during high speed operation, thus at the low speed heavy-haul trains operate at the rolling resistance is the more significant factor.

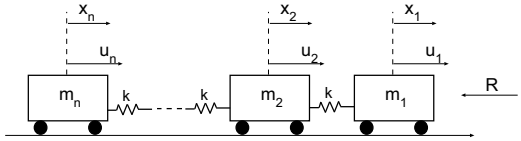

Fig. 2. Force diagram of the train.

The force diagram of a train is shown in figure 2, where n is the number of cars. The equation of motion of the train is

$$\left.\begin{aligned} m_1\ddot{x}_1 &= u_1 - k^-(x_1 - x_2) - \underbrace{(c_0 + c_v\dot{x}_1)}_{R_1^r} m_1 \\ &\quad - \underbrace{c_a\dot{x}_1^2}_{R^a}\Big(\sum_{i=1}^{n} m_i\Big) \\ m_i\ddot{x}_i &= u_i - k^-(x_i - x_{i+1}) - k^-(x_i - x_{i-1}) \\ &\quad - \underbrace{(c_0 + c_v\dot{x}_i)}_{R_i^r} m_i, \quad i = 2, \ldots, n-1 \\ m_n\ddot{x}_n &= u_n - k^-(x_n - x_{n-1}) - \underbrace{(c_0 + c_v\dot{x}_n)}_{R_n^r} m_n \end{aligned}\right\} \tag{3}$$

where $\dot{x}_i$ and x_i are the velocity and the displacement of the car with respect to its own inertial frame; k is the spring constant of the connectors; u_i is the traction force of the car. Note that $u_i \leq 0,\ i = 2, \ldots, n$. This is due to the fact that although the wagons are not powered in a heavy-haul train, they are still able to exert a braking force.

3.2 Open-loop control

In the locomotive lever settings is used to represent different traction power settings. It is, in essence, an open-loop controller that requires the driver to determine the correct power setting for a specific scenario. To find the open loop controller,

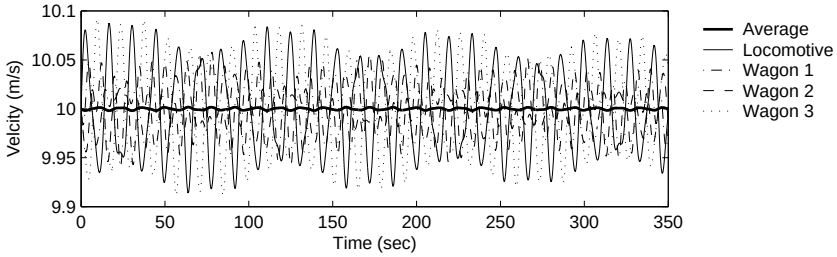

Fig. 3. Velocity of the open-loop system.

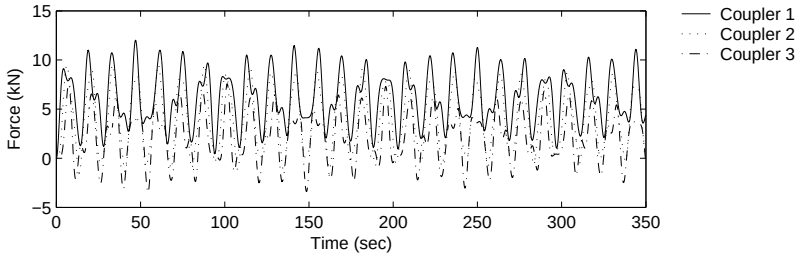

Fig. 4. In-train forces experienced by the open-loop system.

assume the train is in an equilibrium state where the velocity of each car is equal to some cruising speed such that $\dot{x}_i = v_{eq}, \quad i = i, \ldots, n$. Based on the dynamic equations obtained in (3) and letting $\ddot{x}_1 = \ddot{x}_2 = \cdots = \ddot{x}_n = 0$, the control force u_i^e and the position x_i^e can be found as

$$\left.\begin{aligned} u_1^e &= c_0 m_1 + c_v m_1 v_0 + c_a (\sum_{i=1}^{n} m_i) v_0^2 \\ u_n^e &= c_0 m_n + c_v m_n v_0, \quad i = 2, \ldots, n \end{aligned}\right\} \tag{4}$$

$$x_1^e \approx x_2^e \approx \cdots \approx x_n^e \tag{5}$$

where (5) is an approximation since the wagons are not traction powered to sustain the condition $x_n - x_{n-1} = 0$ at the equilibrium state.

In a heavy-haul train only the locomotive has traction. From (4) it can be approximated that the traction force the locomotive will have to exert to maintain the equilibrium velocity will be

$$u_{loco}^e = (c_0 + c_v v_0 + c_a v_0^2) \sum_{i=1}^{n} m_i \tag{6}$$

The regulation performance of the open-loop system is shown in figure 3 and 4. Although the velocities of the cars oscillate continuously, it should be noted that the average velocity of the train system is still maintained around the initial velocity, proving the assumption made in (6) was acceptable.

Figure 4 shows the in-train force experienced by the couplers. Note the in-train force experienced by coupler 1, which connects the locomotive to the rest of the train, is higher than the others. This coincides with the fact that the locomotive is the only source of traction in the train, thus validating the model's ability in providing insights into the coupler force dynamics.

3.3 Closed-loop control

By using (4) and (5) and substituting $x_i = x_i^e + \delta x_i$ and $u_i = u_i^e + \delta u_i$, (3) can be linearised into

$$\left.\begin{aligned} m_1 \delta\ddot{x}_1 &= \delta u_1 - k^-(\delta x_1 - \delta x_2) - (c_0 + c_v \delta\dot{x}_1) m_1 \\ &\quad - 2c_a \delta\dot{x}_1 (\sum_{i=1}^{n} m_i) \\ m_i \delta\ddot{x}_i &= \delta u_i - k^-(\delta x_i - \delta x_{i+1}) \\ &\quad - k^-(\delta x_i - \delta x_{i-1}) - (c_0 + c_v \delta\dot{x}_i) m_i \\ &\quad i = 2, \ldots, n-1 \\ m_n \delta\ddot{x}_n &= \delta u_n - k^-(\delta x_n - \delta x_{n-1}) \\ &\quad - (c_0 + c_v \delta\dot{x}_n) m_n \end{aligned}\right\} \tag{7}$$

The model can be rewritten in a state space form as

$$\dot{\boldsymbol{x}} = \begin{bmatrix} \mathbf{0}_{n\times n} & \mathbf{I}_{n\times n} \\ \mathbf{A}_{21} & \mathbf{A}_{22} \end{bmatrix} \boldsymbol{x} + \begin{bmatrix} \mathbf{0}_{n\times n} \\ \mathbf{B}_{21} \end{bmatrix} \boldsymbol{u} \tag{8}$$

where

$$\mathbf{B}_{21} = \mathbf{I}_{n\times n} \tag{9}$$

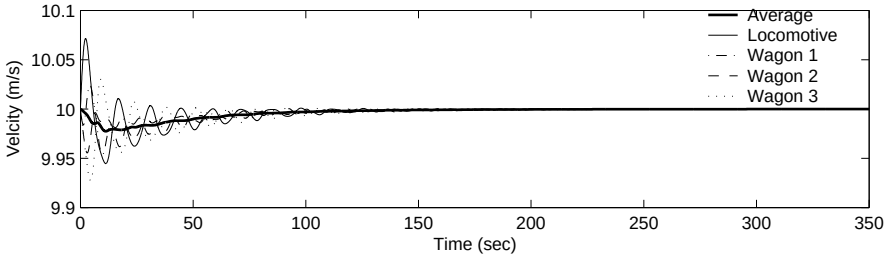

Fig. 5. Velocity of the closed-loop system.

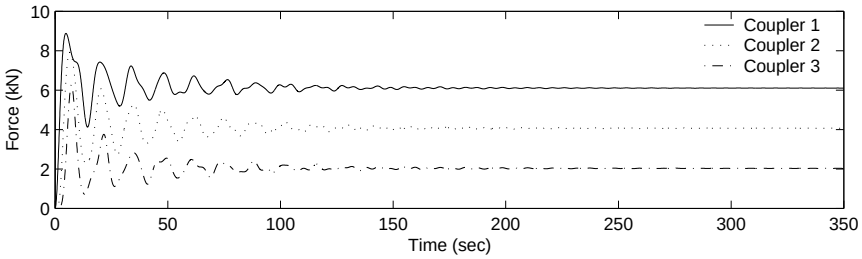

Fig. 6. In-train forces experienced by the closed-loop system.

$$\mathbf{A}_{21} = \begin{bmatrix} \frac{-k^-}{m_1} & \frac{k^-}{m_1} & 0 & \dots & \dots & 0 \\ \frac{k^-}{m_2} & \frac{-2k^-}{m_2} & \frac{k^-}{m_2} & 0 & \dots & 0 \\ 0 & \frac{k^-}{m_3} & \frac{-2k^-}{m_3} & \frac{k^-}{m_3} & \dots & 0 \\ \dots & \dots & \dots & \dots & \dots & \dots \\ 0 & \dots & \frac{k^-}{m_{n-1}} & \frac{-2k^-}{m_{n-1}} & \frac{k^-}{m_{n-1}} & 0 \\ 0 & \dots & \dots & 0 & \frac{k^-}{m_n} & \frac{-k^-}{m_n} \end{bmatrix}_{n\times n} \tag{10}$$

$$\mathbf{A}_{22} = \begin{bmatrix} -c_v - \frac{2c_a v_0 \left(\sum_{i=1}^{n} m_i\right)}{m_1} & 0 & \dots & 0 \\ 0 & -c_v & \dots & 0 \\ 0 & \dots & \dots & 0 \\ 0 & \dots & \dots & -c_v \end{bmatrix}_{n\times n} \tag{11}$$

The state variables $\boldsymbol{x} = [\delta x_1 \ \dots \ \delta x_n \quad \delta\dot{x}_1 \ \dots \ \delta\dot{x}_n]$ and $\boldsymbol{u} = [\delta u_1 \ \dots \ \delta u_n]$ are the deviations from the equilibrium point.

Notes in (8), although there are n inputs, except for the locomotive's control signal u_1, the other control signals can only have a negative value. This is because the wagons only have brakes and cannot be powered. With the new ECP brake system, each wagon would be able to brake independently. This provides additional control inputs as well as flexibility to the system. This means that the brake control signal $u_i,\ i = 2, \dots, n$ are independent and not necessarily equal.

Using state feedback techniques, a feedback gain K was calculated. As the main performance criterion is the velocity tracking, only the feedback gain for the velocities was considered.

The regulation response of the closed-loop system is shown in figure 5 and 6. Both velocity and the in-train force of the closed-loop system show less fluctuation in than the open-loop system responses. While steady velocity translates to energy saving, less fluctuation in the in-train force reduces the chances of metal fatigue in the couplers.

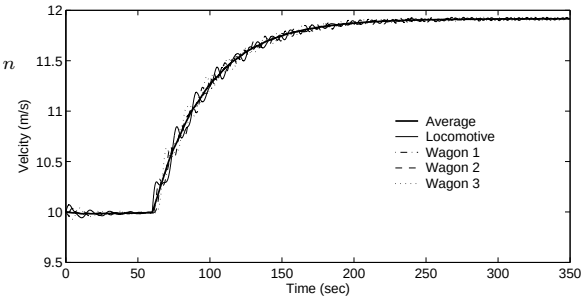

Fig. 7. Velocity step response of the closed-loop system.

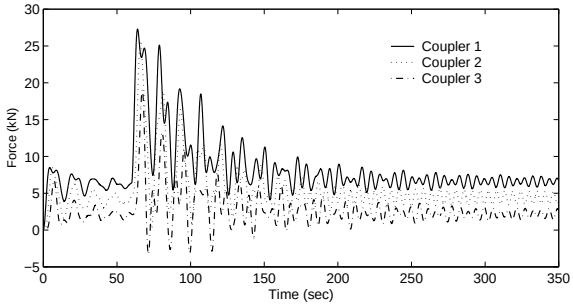

Fig. 8. In-train force step response of the closed-loop system.

The step responses are shown in figure 7 and 8. The reference input was increased from the equilibrium velocity $10ms^{-1}$ to $12ms^{-1}$ at time $60s$.

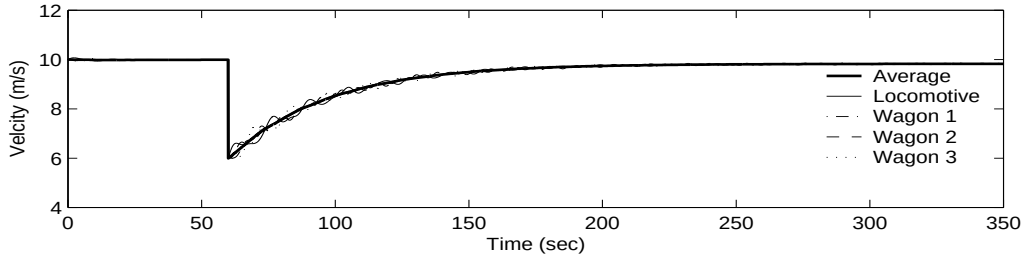

Fig. 9. Velocity response of the closed-loop system with respond to a wind gust disturbance.

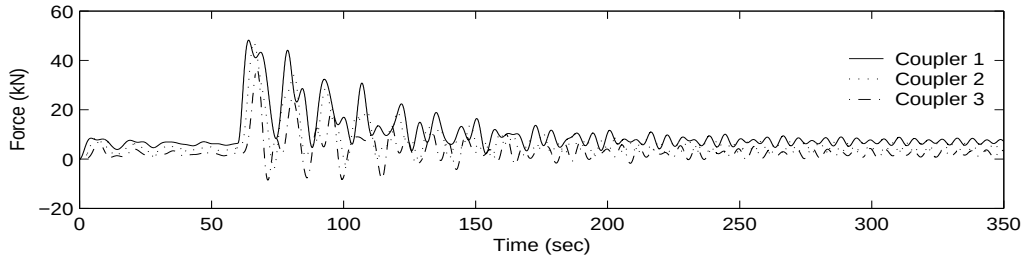

Fig. 10. In-train forces experienced by the closed-loop system with respond to a wind gust disturbance.

The velocities increased smoothly to $11.92ms^{-1}$, a steady state error of 0.7%. The in-train force exhibited a peak value of $27.3kN$, experienced by coupler 1, during the transient phase. The steady-state in-train force values did not vary noticeably, although slightly smaller oscillations occurred.

3.4 Disturbance performance

The closed-loop system was subjected to a head-on wind gust of $4ms^{-1}$ output disturbance at $t = 60s$. The velocity of train recovers asymptotically to $9.825ms^{-1}$, a steady state error of 1.75%. The in-train force peaked just below $50kN$ soon after the wind gust was applied, stabilising at the same time the velocities stabilise. In comparison with the step response, the change in velocity was twice as large. But since both systems reached stable velocity around the same time, it means the acceleration doubled in this case, which accounts for the large increase in the peak in-train force.

4. CONCLUSION

This paper has provided suggestions for two out of the three main running cost factors of a heavy-haul train: energy consumption and travelling time. In-train force, the third cost factor, was investigated through both open-loop and closed-loop control design.

Some observations with regard to in-train force can be made from the results. Firstly, certain amount of in-train forces always exists in the couplers, even at cruising velocity. Next, in-train forces are greatest at the coupler between the locomotive and the first wagon, and decreases sequentially down the train. Lastly, in-train forces are approximately directly proportional to the acceleration rate of the train.

Three conclusions are obtained from this study. First, in-train forces can be effectively controlled via velocity regulation. Secondly, state feedback design is capable of reducing in-train force and velocity regulation. Lastly, acceleration of the feedback system is proportional to the magnitude of the reference input.

The feedback controller still has rooms for improvement; the minor steady error, possibly due to model uncertainties, needs to be addressed; the acceleration rate should be limited to avoid large peaks in the in-train forces; better control on the in-train force. Once updated, the feedback controller, combined with the optimal control method, could provide an all-round solution that targets all three running cost factors at once. Different controllers must be developed for different track and operational conditions.

REFERENCES

Howlett, P. (1996). Optimal strategies for the control of a train. *Automatica* **32**(4), 519–532.

Ishikawa, Y. and A. Kawamura (1997). Maximum adhesive force control in super high speed train. Vol. 2. pp. 951–954.

Watanabe, T. and M. Yamashita (2001). A novel anti-slip control without speed sensor for electric railway vehicles. *The 27th annual conference of the IEEE* **2**, 1382–1387.

Yang, C.D. and Y.P. Sun (2001). Mixed H_2/H_∞ cruise controller design for high speed train. *International Journal of Control* **74**(9), 905–920.